HSPI The Open Access Publisher

J R O JOURNAL OF RADIOLOGY AND ONCOLOGY
ISSN 2573-7724

Research Article

Assessment of using an Octavius 4D Measuring System for Patient-specific VMAT Quality Assurance in Togo

Yawo AC Fiagan[1,2]*, Kodjo JF N'Guessan[3], Adama Diakité[3,4], Komlanvi V Adjenou[3,4], Thierry Gevaert[2,5] and Dirk Verellen[1,6]

[1]Iridium Netwerk, Radiation Oncology, Antwerp, Belgium
[2]Faculty of Medicine and Pharmacy, Vrije Universiteit Brussel, Brussels, Belgium
[3]Department of Radiation Oncology, International Cancer Centre of Lomé, Lomé, Togo
[4]Faculty of Medicine and Pharmacy, University of Lomé, Lomé, Togo
[5]Department of Radiation Oncology, Universitair Ziekenhuis Brussel, Vrije Universiteit Brussel, Belgium
[6]Faculty of Medicine and Health Sciences, Center for Oncological Research (CORE), Integrated Personalized and Precision Oncology Network (IPPON), Universiteit Antwerpen, Antwerp, Belgium

Abstract

Purpose and objective: Quality assurance (QA) programs are designed to improve the quality and the safety of radiation treatments, including machine- and patient-specific QA (PSQA). The objective of this study was to evaluate the current state of PSQA practice and identify the area for potential improvement for VMAT delivery.

Materials and methods: The Octavius 4D (O4D) system accuracy was evaluated using an O4D homogeneous phantom for different field sizes. The system response to dose linearity, field sizes, and PDD difference tests were performed against the calculated dose of the treatment planning system (TPS) for a 6 MV photon beam. The deviation of the delivered dose was evaluated at the isocenter and different depths. Moreover, pretreatment verification of 40 VMAT plans was performed including prostate cancer (PC), head and neck cancer (HNC), uterine and cervical cancer (UCC), and breast cancer (BC). The PTW VeriSoft software was used to perform the local and global 3D gamma analysis by comparing the reconstructed 3D dose against the calculated dose using criteria 2%/2 mm and 3%/3 mm, 20% of low-dose threshold, and 95% of gamma passing rate (%GP) tolerance level. In the clinical scenario, the sensitivity of the O4D system in detecting VMAT delivery and setup errors has been investigated by measuring the variation of %GP values before and after the simulated errors using one of the VMAT plans related to each treatment site.

Results: The O4D system reported good agreement for linearity, field size, and PDD differences with TPS dose being within ± 2% tolerance for a 6 MV photon beam. Output factors were consistent between the ionization chamber and the O4D detector 1500 array down to 4 x 4 cm^2 field size with a maximum deviation of less than 1%. The introduction of deliberate errors caused the decrease of %GP values. In most scenarios, the %GP value of simulated errors was detected with 2%/2 mm and ranged between the detection threshold and gamma passing threshold.

Conclusion: The results indicate that the O4D system is sensitive to detect delivery and setup errors with restrictive criteria of 2%/2 mm for routine pretreatment verification. Moreover, this system should be used in combination with kV-CBCT to improve dosimetry accuracy and treatment reproducibility.

More Information

***Address for correspondences:** Yawo AC Fiagan, PhD Candidate, Iridium Netwerk, Radiation Oncology, GZA Hospitals, Sint-Augustinus-Iridium Netwerk, Oosterveldlaan 24, 2610 Wilrijk, Antwerp, Belgium, Email: Yawo.Fiagan@zas.be

Submitted: July 15, 2024
Approved: September 02, 2024
Published: September 03, 2024

How to cite this article: Fiagan YAC, N'Guessan KJF, Diakité A, Adjenou KV, Gevaert T, Verellen D. Assessment of using an Octavius 4D Measuring System for Patient-specific VMAT Quality Assurance in Togo. J Radiol Oncol. 2024; 8(3): 085-092. Available from: https://dx.doi.org/10.29328/journal.jro.1001070

Keywords: Octavius 4D system; Patient-specific quality assurance; Gamma passing rate; Gamma index

Abbreviations

RT: Radiotherapy; VMAT: Volumetric Modulated Arc Therapy; OAR: Organ At Risk; QA: Quality Assurance; PSQA: Patient-Specific Quality Assurance; HNC: Head and Neck Cancer; UCC: Uterine and Cervical Cancer; PC: Prostate Cancer; BC: Breast Cancer; fx: Fraction; O4D: Octavius 4D; TPS: Treatment Planning System; CCC: Collapsed Cone Convolution; MLC: Multi-Leaf Collimator; kV-CBCT: Kilovoltage Cone Beam Computed Tomography; MU: Monitor Unit; EPID: Electronic Portal Imaging Device; DRR: Digitally Reconstructed Radiograph; IVD: *In vivo* Dosimetry; RTT: Radiation Therapy Technologist; %GP: Gamma Passing Rate; GI: Gamma Index; TV: Target Volume; DTA: Distance-

To-Agreement; DD: Dose Difference; CTV: Clinical Target Volume; PTV: Planning Target Volume; MP: Medical Physicist; PDD: Percent Depth Dose; SSD: Source Surface Distance; TPR: Tissue Phantom Ratio

Introduction

Africa has a population of over 1.2 billion comprising 54 countries, and cancer care services are limited in many of those countries [1]. There are 222 reported RT centers in 29 countries including Togo. The advanced external beam radiotherapy (RT) technique as volumetric modulated arc therapy (VMAT) enables optimal conformal dose distributions to the target volume (TV) while reducing the dose to organs at risk (OARs) [2,3]. This approach can be achieved with one or more arcs by continuously varying the multi-leaf collimator's (MLC) aperture shape, the fluence output rate, and the gantry rotation speed which may yield in reduction of monitor units and treatment time [4]. With the introduction of this complex technique, the inaccuracy, uncertainties, and errors in dose delivery have substantially increased. Moreover, geometrical and anatomical variations can also occur due to weight loss, tumor shrinkage, edema, and postoperative changes during treatment, and it varies from patient to patient [5,6]. For these purposes, comprehensive quality assurance (QA) programs have been introduced including machine-and patient-specific QA (PSQA) to ensure the safety of patients, to prevent clinically relevant errors, and to improve accuracy. This PSQA can be performed before treatment (pretreatment verification) or during the treatment (*in vivo* dosimetry, IVD). Hence, the pretreatment PSQA for VMAT plans has become a current standard of practice [7-10]. Several studies have reported that different pretreatment PSQA can detect different types of errors in VMAT delivery [11]. However, errors due to anatomical variations cannot be detected by employing pretreatment PSQA. Thus, *in vivo* dosimetry is recommended as an additional method for PSQA [12-14]. For geometrical uncertainties, image-guided RT protocols have been introduced to mitigate these errors [15]. The most used clinical metric is the gamma index (GI) analysis which quantifies the difference between measured and calculated dose distributions in terms of dose difference (DD) and distance to agreement (DTA) [16,17]. However, the GI approach is limited by the fact that it only determines the number of points out of tolerance without giving any information about their spatial location. Only recently, Task Group 218 (TG-218) has published guidelines to help streamline the PSQA process and the interpretation of some results [16]. Clinical protocols generally require a gamma pass rate (%GP) higher than 95% for analysis criteria with a 3% - 5% dose difference and 3 mm - 4 mm distance to agreement [18]. However, this has been reported as a challenge in identifying a metric discriminating between passing and failing plans. Several studies have compared various GI analyses and revealed that 3D GI metrics are more efficient because they provide a full volumetric assessment as an alternative to the single-plane 2D GI analysis [19,20].

It is important to know that Togo is a low-income country, and at the time of this retrospective study, there is no legal requirement to carry out PSQA measurements. The RT center is free to follow any guidelines or use any PSQA methods that seem appropriate. Thus, PTW Octavius 4D (O4D) system and VeriSoft software (PTW, Freiburg, Germany) are used for this purpose due to a time-resolved dosimetric acquisition as it rotates together with gantry, and allows the reconstruction of a volumetric dose distribution for high-precision RT. In addition to that, the medical physicist (MP) is not recognized as part of health care professional teams, so the center has an external collaboration with the Senior medical physicists (PMs) group in Europe which is also working with more than 7 countries. The objective of this study was to evaluate the current state of PSQA practice in Togo and identify areas for potential improvement.

Materials and methods

Patient selection and ethics statement

This study retrospectively involved forty patients who underwent RT treatment with the VMAT technique in our institute between January 2023 and June 2024. The study was conducted at the Lomé International Cancer Center (CICL) and approved by the ethics committee. The patient's consent was waived for this PSQA. There were 10 VMAT plans each for patients with head and neck cancer (HNC; with prescribed dose of 70Gy in 2Gy for 35 fractions (fx)), uterine and cervical cancer (UCC, 70Gy, 2.8Gy/25fx), prostate cancer (PC, 74Gy, 2Gy/37fx), and breast cancer (BC, 50Gy, 2Gy/25fx), the most diagnosed cancers in West Africa, particularly in Togo.

Treatment planning and VMAT optimization

All treatments were planned on the pinnacle treatment planning system (TPS, Philips Radiation Oncology Systems, Fitchburg, WI, version 16.2.1) using the Collapsed Cone Convolution (CCC) algorithm for the dose calculation model. The TPS process is semi-automated using the script. All patients were treated with an Elekta Synergy linear accelerator, equipped with a millennium 120 leaf MLC, an EPID system IviewGT, and kV-Cone Beam Computed Tomography (kV-CBCT) imaging systems. The dose was delivered using 6 MV photon beams with a VMAT technique, a maximum dose rate of 600 monitor units (MUs) per minute, and 2° or 4° control-point spacing. Each treatment fraction was delivered with partial arcs or full two arcs due to the tumor size and treatment site without couch rotations. CT images were acquired with a 2.5 mm slice thickness. Target volumes (TVs) and OARs were automatically contoured using ART-Plan™ software. A different margin around the clinical target volume (CTV) was applied to generate PTV according to the treatment site. MOSAIQ record and verify system (Elekta, Stockholm, Sweden) was used in transferring plan parameters to the Linac control system. The online and offline IGRT protocol was applied to ensure precise and

reproducible patient setup. The daily online IGRT protocol included comparing orthogonal kV-kV images with digitally reconstructed radiographs (DRRs) generated from planning CT images for Breast localizations and CBCT for others. Immediate corrective action before each treatment fraction was performed by automated adjustment of the treatment couch in three dimensions when the shift exceeded the action level of 3 mm. If the shift exceeds 2cm then RTTs need to manually adjust the table position with the hand panel inside the bunker. After the couch corrections, MV/kV or CBCT images were acquired for final verification of treatment localization. Plans were calculated with a dose grid of 3 mm. Treatment plans of 40 clinical plans were recalculated on the O4D phantom with the same dose grid. In our center, the plan was considered unacceptable, if the maximum dose (Dmax) to the PTV and near-maximum dose (D2%) to the CTV exceeded 107% and 104% of prescribed doses respectively; if the near-minimum dose (D98%) was lower than 95% of the prescribed dose.

Octavius 4D (O4D) VMAT measurement system

The O4D measuring system is a combination of a phantom and a detector array. It acquires and stores the 2D array measurements as a function of time and gantry angle intervals. This O4D phantom is a motorized cylindrical polystyrene (RW3) phantom, consisting of a water-equivalent plastic with a density of 1.05 g/cm^3, a diameter of 32 cm, and a length of 34.3 cm. It has an insert in the center for a detector array, a trolley for transport that holds the electrometer and the control unit, and a wireless inclinometer that transfers a piece of movement information to the phantom and later acquires dosimetric data. Data are processed by PTW Verisoft software that allows dose evaluation with different metrics. The inclinometer is mounted on the gantry to ensure that the rotation unit always rotates along with the gantry, thus keeping the 2D array perpendicular to the beam axis. All measurements were performed using a detector 1500 array that has a high resolution (dose: 0.1 mGy and dose rate: 0.1 mGy/min), 1405 ionization chambers, each having an entrance area of 4.4 x 4.4 mm^{2,} and a height of 3 mm, resulting in an ionization volume of 58.08 mm^3. The center-to-center spacing is 7.1 mm across a total active area of 27 x 27 cm^2. To achieve absolute dose, the central chamber of the array was cross-calibrated with a PTW semiflex ionization chamber inserted into an RW3 slab phantom replacing the 2D array inside the O4D. Several studies have demonstrated the robustness and accuracy of this phantom [21]. The system was calibrated with a 10 × 10 cm^2 field size with 259.3 MU corresponding to 2Gy at the central ionization chamber.

O4D performance tests

The O4D system was tested for dose linearity and field size dependence. The device dose linearity was tested by delivering a 6 MV with a static field 10 x 10 cm^2 for the variety of MUs (2- 600 MU) at gantry 0°. With very soft software, doses were analyzed at the central ionization chamber of 1500 detector array for each delivered MU and then normalized to the output for 100 MU. The Pearson correlation coefficient was evaluated for linear correlation of doses *vs.* MU.

The field size dependence was evaluated by measuring the output factor for each field size ranging from 2 × 2 to 20 × 20 cm^2 and normalized to 10 × 10 cm^2. For each field size, 100 MU was delivered in the center of the O4D phantom (16 cm depth). For Semiflex ionizing chamber measurements, the RW3 slab phantom was used in the same setup conditions. The same MU was delivered to each field size at SSD = 90 cm and 10 cm depth. Output factors of both detectors were compared (output factor *vs.* MU).

To compare dose variations between the O4D system and TPS, square field sizes ranging from 5 x 5 cm^2 to 25 x 25 cm^2 were planned with TPS using the O4D CT phantom and optimized with the CCC dose calculation algorithm. For each field size, the dose delivery was carried out with a gantry at 0° and 100 MU at isocenter and different depths. The measured dose distributions were analyzed using the VeriSoft software, which is constituted with the output factor, dose profile, and PDD components for each field size. These data were extracted from the Verisoft software by copying the displayed dose profiles at different depths of the detector array to text and importing them into Microsoft Excel for analysis. Dose differences were then calculated relative to the center data point of the detector array.

The reconstruction algorithm accuracy was tested with the same field sizes and dose distributions were analyzed with 2%/2 mm and 3%/3 mm acceptance criteria.

The gamma index and error detectability analysis

The results of the PSQA measurements were analyzed using the GI with VeriSoft software by comparing the reconstructed dose against the 3D dose matrix from the TPS. The 3D GI was calculated using 2%/2 mm and 3%/3 mm acceptance criteria. The center has adopted global 3%/3 mm acceptance criteria as a clinical standard and a 20% low dose threshold. The mean and standard deviation of gamma passing rate (%GP) values were calculated for each criterion and each treatment site in all three axes (transversal, coronal, and sagittal) for global and local absolute normalization.

To test the sensitivity of the O4D system, setup errors were deliberately introduced by shifting the phantom position away from the isocenter. The couch shifted the isocenter to 1 mm, 5 mm, and 10 mm in the left and right axial plane, to 5 mm in the vertical plane, and rotated the isocenter to 1° - 2°. The variation of MU and collimator angle were also simulated by changing throughout rt-plan DICOM files. The collimator was rotated from the isocenter by 1° and 5° and the output of the linac was varied using 2% - 3% MU. GI analysis was evaluated with global 2%/2 mm and 3%/3 mm

by measuring the variation of %GP value before and after the introduction of delivery and setup errors using the same MU for each VMAT plan related to each treatment site except the case of MU variation error scenarios.

Statistical analysis

A paired t-test was used to test for the significance of differences in mean %GP value between global and local GI analysis. A p - value < 0.05 was considered a statistically significant difference. Confidence limit (CL) was also evaluated based on the mean and standard deviation of %GP values for VMAT PSQA related to each treatment site using the following formula: $CL=(100-\%GP_{mean}+1.96\times\sigma\%GP_{mean})$ (1). Therefore, the detection threshold (DT) corresponds to the difference between the expected value of 100% and the confidence limit was also evaluated as follows: $DT = 100-CL$ (2).

Results

For the linearity between the dose measured with the O4D detector system and the output of an Elekta synergy, three measurements were performed for each MU setting and their mean value was plotted against MU using the Pearson correlation approach. The R^2 value was 0.999 with the standard deviation of 0.3 showing that the dose-response of the O4D detector array was linear as shown in Figure 1.

Output factors showed a similar trend between measurements using the O4D detector system and the PTW Semiflex detector. Differences are within 0.7% for 6 MV between field sizes from 4 x 4 cm^2 to 20 x 20 cm^2, but for small field sizes 2 x 2 cm^2 this difference was 1.3%. The results of output factors for both detectors are represented in Figure 2.

All static plans for field size from 5 x 5 cm^2 to 20 x 20 cm^2 were analyzed using the homogenous O4D phantom and acceptance criteria of 2%/2 mm and 3%/3 mm in global and local analysis are reported in Table 1 including the percentage dose difference (%ΔD) at isocenter of the phantom (16 cm depth).

Results of %GP using 3%/3 mm and 2%/2 mm acceptance criteria were greater than 98% and 93 % respectively using global GI analysis for all static fields compared to 97% and 85% respectively for local GI analysis. Results showed a decrease in %GP values for large static field sizes due to some mismatching in the penumbra region at field edges. The comparison of agreement in the three different axes showed a better result on the transversal axis for all static fields. In addition, the percentage dose differences between doses measured with the O4D system and those calculated with TPS were within ±2% accuracy.

Results of PDD differences between the O4D system and TPS showed a maximum dose difference of 1.5% at a depth of 5 cm related to a field size 10 x 10 cm^2. Moreover, the decrease of these PDD differences for each field size of different depths was also observed. The $TPR_{20,10}$ was 0.63 at depths of 20 cm and 10 cm for a field size 20 x 20 cm^2 was less than 1%. The results of PDD differences at different depths are represented in Table 2.

The mean of %GP values and standard deviations using 2%/2mm and 3%/3mm acceptance criteria for VMAT clinical plans were evaluated. The GI calculated concerning the maximum point was significantly higher than the one calculated point by point using our institute standard acceptance criteria 3%/3mm for patients with PC (95.92% *vs.* 88.95%; $p = 0.03$), HNC (93.72% *vs.* 86.20%; $p = 0.02$) and UCC (93.46% *vs.* 84.05%, $p = 0.01$), BC (91.10% *vs.* 80.82%; $p < 0.01$) respectively. However, acceptance criteria 2%/2 mm were too tight causing a significant decrease in the mean %GP value particularly for local GI evaluation. The results evaluated on the three axes showed a better agreement on the transversal axis for all VMAT plans and results are reported in Table 3.

The error detection threshold was evaluated only for global GI evaluation including the mean of % GP value, standard deviation, and confidence limit. Results showed that the DT for all treatment sites was higher than 85% for

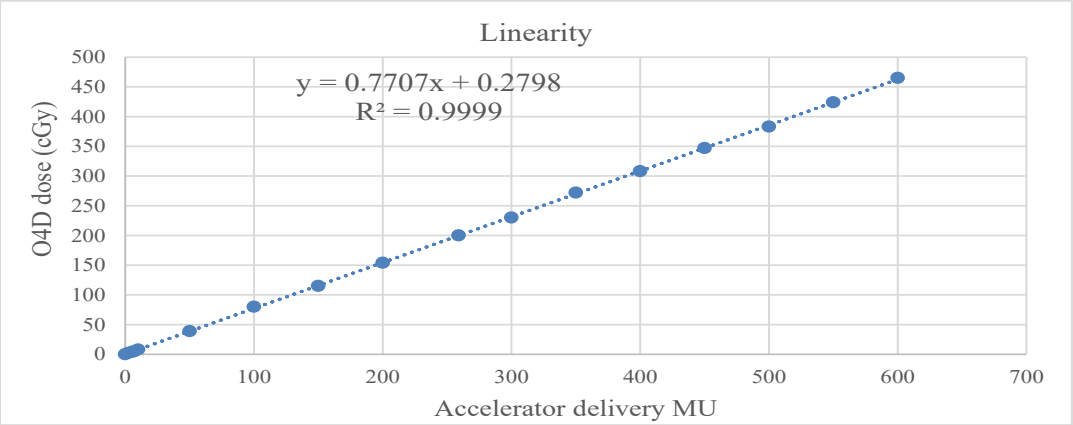

Figure 1: Linearity between the O4D detector system measured dose and Elekta synergy delivery MU.

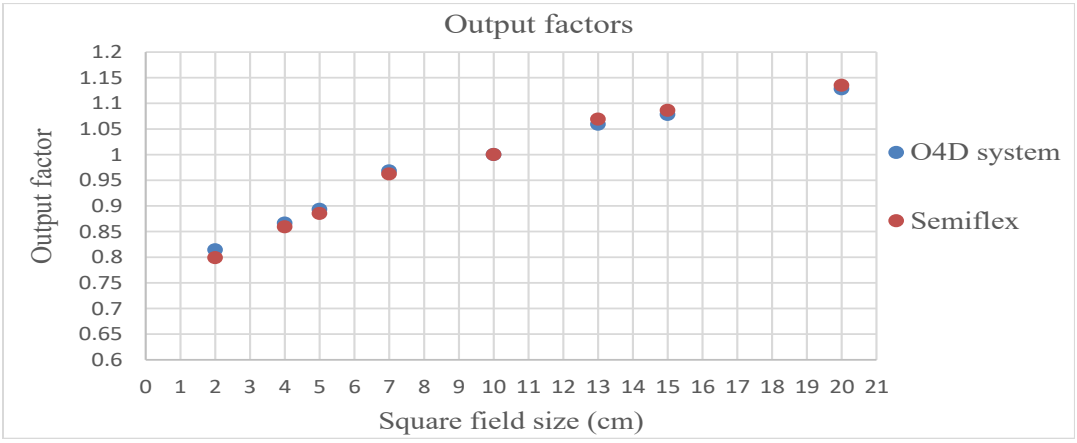

Figure 2: Results of output factor measured with O4D detector array (in blue) and Semiflex detector (in red).

Table 1: 3D gamma results for different static fields in three directions and percentage dose difference (%ΔD) at isocenter.

Field size (cm x cm)	Direction	3D Global GPR		3D local GPR		
		2%/2 mm	3%/3 mm	2%/2 mm	3%/3 mm	%ΔD
5 x 5	Transversal	99.9	100	99.7	100	0.9
	Sagittal	99.8	100	99.6	100	
	Coronal	99.8	100	99.6	100	
10 x 10	Transversal	99.8	100	98.8	99.9	0.3
	Sagittal	99.7	100	97.6	99.8	
	Coronal	99.7	100	97.4	99.7	
15 x 15	Transversal	97.8	99.9	95.8	98.6	-0.6
	Sagittal	96.6	99.8	95.4	98.4	
	Coronal	96.5	99.8	95.2	98.2	
20 x 20	Transversal	95.2	98.7	85.7	97.8	-0.8
	Sagittal	94.6	98.5	85.5	97.5	
	Coronal	93.2	98.2	85.4	97.2	

Table 2: Difference (%) in PDD at different depths and field sizes between the O4D system and TPS using homogenous phantom.

Field size (cm x cm)	PDD difference (%) for different depths			
	5 cm	10 cm	15 cm	20 cm
5 x 5	0.9	0.6	0.5	0.4
10 x 10	1.5	1.2	0.8	0.3
15 x 15	1.3	0.9	0.7	0.3
20 x 20	1.1	0.8	0.6	0.5
25 x 25	1	0.9	0.7	0.6

3%/3 mm and 80% for 2%/2 mm. The results are reported in Table 4.

The simulated errors caused the decrease of %GP values in most scenarios. These errors were detected if the %GP of simulated error was below DT or between the DT and gamma passing tolerance. However, the %GP value of simulated errors above the passing tolerance was considered not detectable. The lateral shift of 1 mm and 5 mm, the vertical shift of 5 mm, 1°, and 2° couch rotation, 2° collimator rotation, and 2% MU variation were not detected in four cases using 3%/3 mm. By using more restrictive criteria of 2%/2 mm, they can be detected except for 1mm shift and 1° couch rotation. All results are represented in Figures 3, 4 respectively.

Table 3: Results of mean %GP and standard deviation using 3%/3 mm and 2%/2 mm acceptance criteria for different pathologies in our center.

Pathology	Gamma index	Direction	2%/2 mm	3%/3 mm
			Mean ± SD	Mean ± SD
Prostate cancer (PC)	3D global	Transversal	**92.87 ± 4.65**	**96.43 ± 2.25**
		Sagittal	**91.79 ± 4.26**	**95.79 ± 2.34**
		Coronal	**91.33 ± 4.18**	**95.53 ± 2.23**
	3D local	Transversal	80.94 ± 5.12	89.86 ± 4.89
		Sagittal	79.22 ± 5.41	88.46 ± 4.67
		Coronal	79.13 ± 5.20	88.52 ± 4.31
Head and neck cancer (HNC)	3D global	Transversal	**91.45 ± 4.79**	**94.85 ± 2.56**
		Sagittal	**90.23 ± 4.21**	**93.25 ± 2.47**
		Coronal	**90.02 ± 4.13**	**93.06 ± 2.43**
	3D local	Transversal	78.26 ± 5.86	86.97 ± 4.95
		Sagittal	77.48 ± 5.50	85.87 ± 4.81
		Coronal	77.03 ± 5.21	85.76 ± 4.79
Uterine and cervical cancer (UCC)	3D global	Transversal	**90.93 ± 4.71**	**93.77 ± 3.75**
		Sagittal	**89.54 ± 4.25**	**93.39 ± 3.36**
		Coronal	**88.74 ± 4.17**	**93.23 ± 3.23**
	3D local	Transversal	75.94 ± 5.12	84.86 ± 4.65
		Sagittal	74.22 ± 4.84	83.76 ± 4.27
		Coronal	74.13 ± 4.20	83.54 ± 4.21
Breast cancer (BC)	3D global	Transversal	**89.94 ± 4.32**	**93.65 ± 3.49**
		Sagittal	**88.76 ± 3.86**	**92.59 ± 3.25**
		Coronal	**88.23 ± 4.23**	**92.06 ± 3.22**
	3D local	Transversal	74.64 ± 5.72	81.86 ± 4.76
		Sagittal	73.22 ± 5.46	80.46 ± 4.37
		Coronal	73.13 ± 5.09	80.14 ± 4.21

Table 4: Results of the confidence limits and threshold error detection for global analysis using 2%/2 mm and 3%/3 mm acceptance criteria.

Pathology	GA	Mean (%)	SD (%)	CL (%)	DT (%)
PC	2%/2 mm	92	4.36	16.56	83.44
HNC		90.57	4.38	18.01	81.99
UCC		89.71	4.55	19.22	80.78
BC		88.98	4.14	19.13	80.87
PC	3%/3 mm	95.92	2.27	8.53	91.47
HNC		93.72	2.49	11.15	88.85
UCC		93.43	3.45	13.33	86.67
BC		92.43	3.32	14.07	85.93

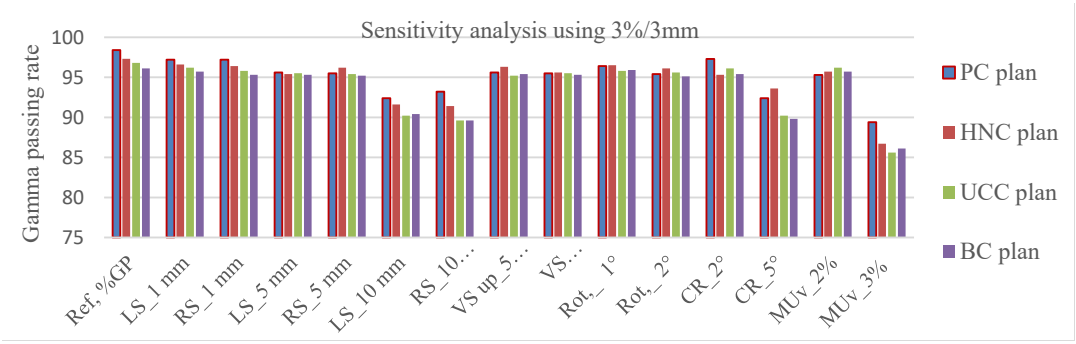

Figure 3: %GP value of VMAT plans for simulated setup and delivery errors using 3%/3 mm and 95% passing threshold. RS: Right Shift of couch; LS: Left Shift of couch; VS: Vertical Shift of couch; Rot: Couch Rotation Angle; CR: Collimator Rotation and MUv=Monitor Unit variation

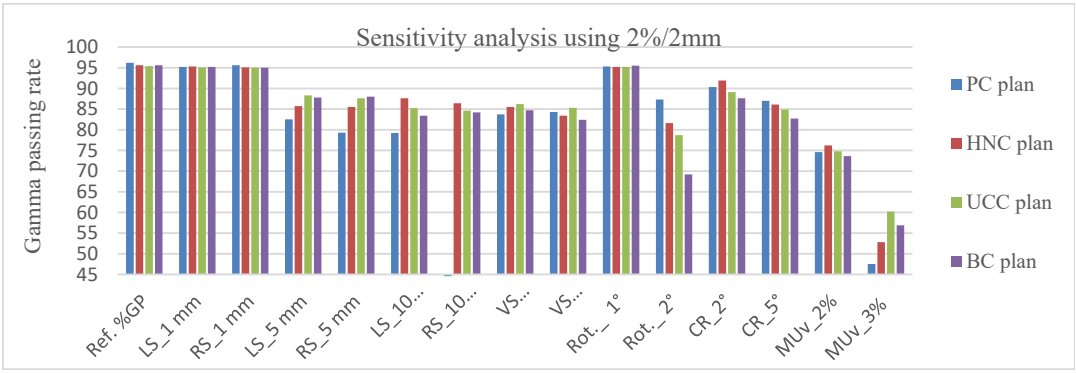

Figure 4: %GP value of VMAT plans for simulated setup and delivery errors using 2%/2 mm and 95% passing threshold.

Discussion

The accuracy and sensitivity of the O4D system were investigated for routine pretreatment verification in the new RT center in Togo. For this paper, two approaches were used to estimate the accuracy of the measured dose distribution in the homogeneous O4D phantom such as the comparison of static field results and clinical VMAT plan results with results of the TPS calculation. Phantom measurements performed with the O4D system demonstrated very good linearity at the central axis for all delivered MUs (Figure 1). Moreover, output factors were consistent between the ionization chamber and the O4D detector 1500 array down to 4 x 4 cm^2 field size with a maximum deviation less than 1% which agrees well with the results of Stelljes, et al. [22]. For all field sizes, the differences between the dose measured with the O4D system and the dose calculated with the TPS were within 2% accuracy. Thus, this ensures the correct implementation of PDDs used for the reconstruction of 3D doses and accurate field size response of the O4D detector system. It should be noted that the accuracy of the O4D system relies on the accuracy of the inclinometer to ensure that the detector array is always perpendicular to the incident beam. Before the O4D detector system is used for PSQA measurements, a calibration is often required to convert the measured reading to the absolute dose. In addition, the O4D system is dosimetrically and mechanically stable because it is always warmed with 800 MU [23]. To ensure the optimal and accurate performance of the PSQA detector and software, regular quality control (QC) is performed.

On the other hand, the accuracy of the O4D system was also investigated using clinical VMAT plans utilizing a GI evaluation approach which showed a good dosimetric agreement between calculated and measured 3D dose distributions using a global 3%/3 mm and 95% passing threshold. Results revealed that the mean %GP values for global 3D GI analysis are quite higher than the mean %GP values for local 3D GI analysis for all treatment sites. These results are consistent with the results reported by Urso, et al. [24] who emphasized that the global normalization is calculated concerning the value of the maximum dose and produced homogenous results with higher %GP. Das, et al. have observed a significant correlation between the local and global gamma index and pointed out that it strongly depends on the dosimetric verification system and the resolution of the detector used [25]. Results also indicated a dependence on the axe where the plan was evaluated and showed that the transversal axis was linked to a better agreement if compared with the coronal and the sagittal axes. This behavior was already highlighted by Urso, et al. who reported that the transversal view is most easily related to the treatment plan isodose on the transversal CT slice of the patient [24]. Our results coincided with a previous work of Esposito, et al. [26]

who evaluated dosimetric check with Octavius 4D phantom measurements for 20 VMAT plans including head and neck and prostate cases, and obtained a mean %GP (3%/3 mm) of 95.6% (±2.5%) with 10% dose threshold.

The sensitivity of the O4D system in detecting deliberate errors from the dose delivery and patient setup was also investigated based on variations of %GP values and detectability threshold to determine which criteria are more appropriate for routine pretreatment verification. The results indicated that the criteria 3%/3 mm with a threshold of 95% masked certain errors caused by deliberate MU errors of 2%, couch rotation angles of 1° and 2°, and lateral (left and right) et vertical (up and down) shift of 5 mm and collimator rotation of 2°. However, these errors were detectable using more restrictive acceptance criteria of 2%/2mm with a 95% threshold (Figure2) except for 1mm couch shift and 1° couch rotation. For deliberate MU errors of 2%, these results were in close agreement with the results reported by Bresciani, et al. [27] who emphasized in the clinical scenario that dose output variations to the VMAT plans of 1% or 2% could not be detected until very strict gamma criteria 1%/1mm were applied. It was observed that the %GP value significantly decreased if 5% MU, 10 mm of left and right lateral shift errors, and 5° collimator rotation were simulated for the VMAT plan related to each treatment site. The O4D system was less sensitive to setup errors and delivery errors when the standard 3%/3 mm was used. Moreover, setup errors can be corrected by using the IGRT protocol to mitigate the residual intra-fractionation displacements and rotations. Based on these results, the acceptance criteria 2%/2 mm could be relevant for routine pretreatment verification in our center.

In case of VMAT plan failure, the medical physicist systematically reviewed the dose difference, distance-to-agreement, gamma index, isodose distribution, dose profile, and structure-specific dose distribution to determine if the dose deviations are clinically relevant. Further analyses were performed to determine the root causes and reasons for these discrepancies to find an appropriate solution. For failed plans due to the more complex modulation, replanning can be considered with less complex intensity patterns. However, the O4D system was limited to the pretreatment verification which becomes a serious challenge to enhance accuracy. Moreover, there is an additional source of uncertainty introduced by anatomical variations. Esposito, et al. [26] and Mijnheer, et al. [11] reported that EPID-based IVD (EIVD) is the only tool able to verify the actual patient treatment, particularly about patient anatomy and possible obstructions from positioning or immobilization devices [26]. It can be used to assess and record the delivered patient dose over a series of treatment fractions without additional cost in measurement time and increase the synergy between RTT, medical physicists, and radiation oncologists. By performing EIVD, systematic morphological changes, due to tumor shrinkage, patient weight loss, and edema, could benefit from adaptive strategies [28]. As a center is using a script to automate much of the pinnacle TPS process and has an Elekta view a-Si EPID, hence EIVD dosimetry can be an optimal solution to enhance this accuracy. Recently, Fiagan, et al. have demonstrated automated EIVD potential to identify changes in patient anatomy, patient setup, beam delivery, and imager position and can help to trigger adaptive radiation therapy [28-31].

However, our study has some limitations. Firstly, the dosimetric impact of introduced errors was not quantified by using DVH software because the center did not have the license for this option. Secondly, the study is a single institute study with a limited sample size, a multi-centered study involving multiple institutions in West Africa could be required to generalize the clinical applicability in PSQA for a high-precision RT.

Conclusion

The results indicate that the Octavius 4D system is sensitive to detect delivery and setup errors with restrictive criteria of 2%/2 mm for routine pretreatment verification. Moreover, this system should be used in combination with kV-CBCT to improve dosimetry accuracy and treatment reproducibility. Subsequently, each institution should establish its own GI analysis protocol including appropriate acceptance criteria with its own linac and detector array.

Acknowledgment

We sincerely thank the CICL for providing logistical support for this work. The authors would like to acknowledge the radiation oncologists, radiation therapists, and medical physicists for their cooperation.

References

1. Yorke AA, Williams VM, Elmore S, Alleyne-Mike K, Addison E, Kyeremeh PO Jr, et al. Radiation Therapy Physics Quality Assurance and Management Practices in Low- and Middle-Income Countries: An Initial Pilot Survey in Six Countries and Validation Through a Site Visit. Adv Radiat. Oncol. 2024;9(2):101335. Available from: https://doi.org/10.1016/j.adro.2023.101335

2. Ezzell GA, Galvin JM, Low D, Palta JR, Rosen I, Sharpe MB, et al. IMRT subcommittee; AAPM Radiation Therapy Committee. Guidance document on delivery, treatment planning, and clinical implementation of IMRT: report of the IMRT Subcommittee of the AAPM Radiation Therapy Committee. Med Phys. 2003;30:2089-115. Available from: https://doi.org/10.1118/1.1591194

3. Otto K. Volumetric modulated arc therapy: IMRT in a single gantry arc. Med Phys. 2008; 35:310-7. Available from: https://doi.org/10.1118/1.2818738

4. Rajasekaran D, Jeevanandam P, Sukumar P, Ranganathan A, Johnjothi S, Nagarajan V: A study on the correlation between plan complexity and gamma index analysis in patient-specific quality assurance of volumetric modulated arc therapy. Rep Pract. Oncol Radiother. 2015; 20(1):57-65. Available from: https://doi.org/10.1016/j.rpor.2014.08.006

5. Barker Jr JL, Garden AS, Ang KK, O'Daniel JC, Wang H, Court LE, et al. Quantification of volumetric and geometric changes occurring

during fractionated radiotherapy for head-and-neck cancer using an integrated CT/linear accelerator system. Int J Radiat Oncol Biol Phys 2004; 59:960-970. Available from: https://doi.org/10.1016/j.ijrobp.2003.12.024

6. Mali SB. Adaptive Radiotherapy for Head Neck Cancer. J Maxillofac Oral Surg. 2016;15:549-554. Available from: https://doi.org/10.1007/s12663-016-0881-y

7. Galvin JM, Ezzell G, Eisbrauch A, Yu C, Butler B, Xiao Y, et al. American Society for Therapeutic Radiology and Oncology; American Association of Physicists in Medicine. Implementing IMRT in clinical practice: a joint document of the American Society for Therapeutic Radiology and Oncology and the American Association of Physicists in Medicine. Int J Radiat Oncol Biol Phys. 2004; 58(5):1616-1634. Available from: https://doi.org/10.1016/j.ijrobp.2003.12.008

8. Tang D, Yang Z, Dai X, Cao Y. Evaluation of Delta4DVH Anatomy in 3D Patient-Specific IMRT Quality Assurance. Technol Cancer Res Treat. 2020;19. Available from: https://doi.org/10.1177/1533033820945816

9. Chan GH, Chin LCL, Abdellatif A, Bissonnette JP, Buckley L, Comsa D, et al. Survey of patient-specific quality assurance practice for IMRT and VMAT. J Appl Clin Med Phys. 2021;22(7):155-164. Available from: https://doi.org/10.1002/acm2.13294

10. Pulliam KB, Huang JY, Howell RM, Followill D, Bosca R, O'Daniel J, Kry SF. Comparison of 2D and 3D gamma analyses. Med Phys. 2014;41(2). Available from: https://doi.org/10.1118/1.4860195

11. Mijnheer B, Jomehzadeh A, González P, Olaciregui-Ruiz I, Rozendaal R, Shokrani P, et al. Error detection during VMAT delivery using EPID-based 3D transit dosimetry. Phys Med. 2018;54:137-145. Available from: https://doi.org/10.1016/j.ejmp.2018.10.005

12. Miften M, Olch A, Mihailidis D, Moran J, Pawlicki T, Molineu A, et al. Tolerance limits and methodologies for IMRT measurement-based verification QA: Recommendations of AAPM Task Group No. 218. Med Phys. 2018;45(4):e53-e83. Available from: https://doi.org/10.1002/mp.12810

13. Bossuyt E, Weytjens R, Nevens D, De Vos S, Verellen D. Evaluation of automated pre-treatment and transit in-vivo dosimetry in radiotherapy using empirically determined parameters. Phys Imaging Radiat. Oncol. 2020;16:113-129. Available from: https://doi.org/10.1016/j.phro.2020.09.011

14. Persoon LC, Podesta M, Nijsten SM, Troost EG, Verhaegen F. Time-Resolved Versus Integrated Transit Planar Dosimetry for Volumetric Modulated Arc Therapy: Patient-Specific Dose Differences During Treatment, a Proof of Principle. Technol Cancer Res Treat. 2016;15(6):NP79-NP87. Available from: https://doi.org/10.1177/1533034615617668

15. Abubakar A, Zamri NAM, Shaukat SI, Mohd ZH. Automated algorithm for calculation of setup corrections and planning target volume margins for offline image-guided radiotherapy protocols. J Appl Clin Med Phys. 2021;22(7):137-146. Available from: https://doi.org/10.1002/acm2.13291

16. Low DA, Harms WB, Mutic S, Purdy JA. A technique for the quantitative evaluation of dose distributions. Med Phys.1998; 25:656-661. Available from: https://doi.org/10.1118/1.598248

17. Stasi M, Bresciani S, Miranti A, Maggio A, Sapino V, Gabriele P. Pretreatment patient-specific IMRT quality assurance: a correlation study between gamma index and patient clinical dose volume histogram. Med Phys. 2012;39(12):7626-7634. Available from: https://doi.org/10.1118/1.4767763

18. Besserer J, et al. Quality control for Intensity-modulated radiation therapy. SSRMP Rec. 2007;15.

19. Pulliam KB, Huang JY, Howell RM, Followill D, Bosca R, O'Daniel J, Kry SF. Comparison of 2D and 3D gamma analyses. Med Phys. 2014; 1(2):021710. Available from: https://doi.org/10.1118/1.4860195

20. Song JH, Kim MJ, Park SH, Lee SR, Lee MY, Lee DS, et al. Gamma analysis dependence on specified low-dose thresholds for VMAT QA. J Appl Clin Med Phys. 2015;16: 263-272. Available from: https://doi.org/10.1120/jacmp.v16i6.5696

21. Stathakis S, Myers P, Esquivel C, Mavroidis P, Papanikolaou N. Characterization of a novel 2D array dosimeter for patient-specific quality assurance with volumetric arc therapy. Med Phys. 2013; 40(7):071731. Available from: https://doi.org/10.1118/1.4812415

22. Stelljes TS, Harmeyer A, Reuter J, Looe HK, Chofor N, Harder D, Poppe B. Dosimetric characteristics of the novel 2D ionization chamber array OCTAVIUS Detector 1500. Med Phys. 2015;42(4):1528-37. Available from: https://doi.org/10.1118/1.4914151

23. Srivastava RP, Basta K, Thevissen K, Junius S, Vandeputte K, De Wagter C. Gamma evaluation with Octavius 4D phantom for pretreatment of modern radiotherapy treatment techniques. International journal of nuclear medicine & Radioactive Substances. 2019;2(2). Available from: http://hdl.handle.net/1854/LU-8675740

24. Urso P, Lorusso R, Marzoli L, Corletto D, Imperiale P, Pepe A, et al. Practical application of Octavius® -4D: Characteristics and criticalities for IMRT and VMAT verification. J Appl Clin Med Phys. 2018;19(5):517-524. Available from: https://doi.org/10.1002/acm2.12412

25. Das S, Kharade V, Pandey VP, Kv A, Pasricha RK, Gupta M. Gamma Index Analysis as a Patient-Specific Quality Assurance Tool for High-Precision Radiotherapy: A Clinical Perspective of Single Institute Experience. Cureus. 2022;14(10): e30885. Available from: https://doi.org/10.7759/cureus.30885

26. Esposito M, Bruschi A, Bastiani P, Ghirelli A, Pini S, Russo S, et al. Characterization of EPID software for VMAT transit dosimetry. Australas Phys Eng Sci Med. 2018;41(4):1021-1027. Available from: https://doi.org/10.1007/s13246-018-0693-0

27. Bresciani S, Poli M, Miranti A, Maggio A, Di Dia A, Bracco C, et al. Comparison of two different EPID-based solutions performing pretreatment quality assurance: 2D portal dosimetry versus 3D forward projection method. Phys Med. 2018;52:65-71. Available from: https://doi.org/10.1016/j.ejmp.2018.06.005

28. Fiagan YAC, Bossuyt E, Nevens D, Machiels M, Chiairi I, Joye I, et al. The use of in-vivo dosimetry to identify head and neck cancer patients needing adaptive radiotherapy. Radiother Oncol. 2023;184:109676. Available from: https://doi.org/10.1016/j.radonc.2023.109676

29. Fiagan YAC, Bossuyt E, Nevens D, Dirix P, Theys F, Gevaert T et al. In vivo dosimetry for patients with prostate cancer to assess possible impact of bladder and rectum preparation. Tech Innov Patient Support Radiat Oncol. 2020;16:65-69. Available from: https://doi.org/10.1016/j.tipsro.2020.10.005

30. Fiagan YAC, Bossuyt E, Machiels M, Nevens D, Billiet C, Poortmans P, et al. Comparing treatment uncertainty for ultra- vs. standard-hypofractionated breast radiation therapy based on in-vivo dosimetry. Phys Imaging Radiat Oncol. 2022;22:85-90. Available from: https://doi.org/10.1016/j.phro.2022.05.003

31. Bossuyt E, Weytjens R, Nevens D, De Vos S, Verellen D. Evaluation of automated pre-treatment and transit in-vivo dosimetry in radiotherapy using empirically determined parameters. Phys Imaging Radiat Oncol. 2020;16:113-129. Available from: https://doi.org/10.1016/j.phro.2020.09.011